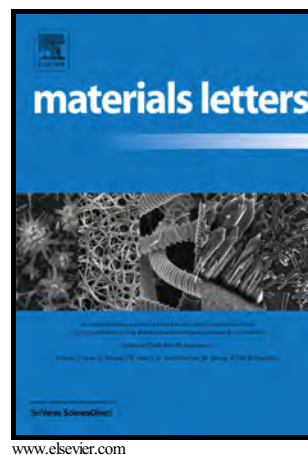


Characterization and microwave dielectric properties of new low loss  $\text{Li}_2\text{MgZrO}_4$  ceramics

J.X. Bi, C.F. Xing, X.S. Jiang, C.H. Yang, H.T. Wu



PII: S0167-577X(16)31352-0  
DOI: <http://dx.doi.org/10.1016/j.matlet.2016.08.067>  
Reference: MLBLUE21351

To appear in: *Materials Letters*

Received date: 27 April 2016  
Revised date: 7 July 2016  
Accepted date: 13 August 2016

Cite this article as: J.X. Bi, C.F. Xing, X.S. Jiang, C.H. Yang and H.T. Wu, Characterization and microwave dielectric properties of new low loss  $\text{Li}_2\text{MgZrO}_4$  ceramics, *Materials Letters* <http://dx.doi.org/10.1016/j.matlet.2016.08.067>

This is a PDF file of an unedited manuscript that has been accepted for publication. As a service to our customers we are providing this early version of the manuscript. The manuscript will undergo copyediting, typesetting, and review of the resulting galley proof before it is published in its final citable form. Please note that during the production process errors may be discovered which could affect the content, and all legal disclaimers that apply to the journal pertain.

School of Materials Science and Engineering, University of Jinan, Jinan 250022, China

\*Corresponding author: Tel.: +86 531 82769782; fax: +86 531 87974453. mse\_wuht@ujn.edu.cn

## Abstract

Low loss microwave dielectric materials  $\text{Li}_2\text{MgZrO}_4$  were synthesized by solid-state route. The relationship among sintering characteristics, phase composition, microstructure and microwave dielectric properties of  $\text{Li}_2\text{MgZrO}_4$  ceramics were firstly investigated using X-Ray Diffraction, Scanning Electron Microscopy and Network Analyzer. The formation of secondary phases and evaporation of lithium were observed when sintering temperatures exceeded  $1175^\circ\text{C}$ . Microwave dielectric properties of  $\text{Li}_2\text{MgZrO}_4$  ceramics were affected by sintering characteristics and second phase. In addition, the bond energy of  $\text{Li}_2\text{MgZrO}_4$  ceramics was also reported to analyze intrinsic loss. Typically, the ceramics sintered at  $1175^\circ\text{C}$  for 4h exhibited excellent microwave dielectric properties with  $\epsilon_r=12.30$ ,  $Q\cdot f=40,900$  GHz and  $\tau_f=-12.31$  ppm/ $^\circ\text{C}$ .

**Keywords:** Ceramics;  $\text{Li}_2\text{MgZrO}_4$ ; Electronic materials; Microwave dielectric properties; Bond energy

## 1. Introduction

Microwave dielectric materials such as duplexers, resonators, antennas, and oscillators play an important role in the rapid growth of mobile and satellite communications [1-3]. For these high frequency wireless communication applications, the microwave dielectric materials should possess high dielectric constant for miniaturization of electronic components, high quality factor for maximum signal intensity and near-zero temperature coefficient of resonant frequency for adaptation to environmental change [4, 5]. Recently, many compounds based on  $\text{Li}_2\text{O-MgO-BO}_2$  (B=Ti, Sn, Zr) system were reported for the possible use in microwave communications [6-8]. Among several kinds of microwave dielectric ceramics, the rock-salt-structured  $\text{Li}_2\text{MgTiO}_4$  ceramics possess a high quality factors and an appropriate dielectric constant, which are suitable candidate materials for contemporary miniaturized and integrated passive components application [9, 10]. For example, Huang et al. reported the microwave dielectric properties of  $\text{Li}_2\text{MgTiO}_4$  ceramics were  $\epsilon_r=17.25$ ,  $Q\cdot f=97,300$  GHz and  $\tau_f=-27.2$  ppm/ $^\circ\text{C}$  when sintered at  $1360^\circ\text{C}$  for 2 h [9]. As for  $\text{Li}_2\text{MgZrO}_4$ , M. Castellanos et al. reported that the  $\text{Li}_2\text{MgZrO}_4$  powders sintered at  $1050^\circ\text{C}$  had the rock-salt structure with the space group of  $I41/amd$ , which had same structure as  $\alpha\text{-LiFeO}_2$  and different structure from  $\text{Li}_2\text{MgTiO}_4$  [11]. However, at present there were no reports of microwave dielectric properties of  $\text{Li}_2\text{MgZrO}_4$  ceramics. In this work, the sintering characteristics, bond energy and microwave dielectric properties of the  $\text{Li}_2\text{MgZrO}_4$  ceramics were investigated. In addition, the relationships among phase composition, microstructure, sintering characteristics and microwave dielectric properties of  $\text{Li}_2\text{MgZrO}_4$  ceramics were also detailed.

## 2. Experimental procedure

The ceramics were prepared by the conventional solid-state route using  $\text{Li}_2\text{CO}_3$  (99.99%),  $\text{MgO}$  (99.99%) and  $\text{ZrO}_2$  (99.9%) as starting materials according to the formula of  $\text{Li}_2\text{MgZrO}_4$ . The mixed powders were milled for 24h with distilled water in a nylon container with  $\text{ZrO}_2$  balls. All the slurries were dried and calcined at  $1050^\circ\text{C}$  for 4h to obtain a single phase of  $\text{Li}_2\text{MgZrO}_4$ . The calcined powders were milled for another 24h and dried. The dried powders were mixed with polyvinyl alcohol as a binder, granulated and pressed into cylindrical disks of 10 mm diameter and about 6 mm height at a pressure of about 200 MPa. These resultant pellets were preheated at  $500^\circ\text{C}$  for 4h to expel the binder and sintered at  $1125\text{-}1225^\circ\text{C}$  for 4h in air at a heating rate of  $5^\circ\text{C}/\text{min}$ .

Phase analysis of samples was conducted with the help of a Rigaku diffractometer using Ni filtered  $\text{CuK}\alpha$  radiation ( $\lambda=0.1542\text{ nm}$ ) at 40 kV and 40 mA settings. To investigate the crystal structure of  $\text{Li}_2\text{MgZrO}_4$ , the X-ray diffraction patterns were analyzed by the Rietveld refinement [12]. The microstructures were examined using a scanning electron microscope. The apparent densities of the sintered pellets were measured using the Archimedes method. A network analyzer was used for the measurement of microwave dielectric properties. Dielectric constants were measured using Hakki-Coleman post-resonator method by exciting the TE011 resonant mode of dielectric resonator by using an electric probe as suggested by Hakki and Coleman [13]. Unloaded quality factors were measured using TE01d mode by the cavity method [14], which could eliminate additional losses caused by parasitic effects. All measurements were made at room temperature and in the frequency of 8-12 GHz. The temperature coefficient of the resonant frequency ( $\tau_f$ ) was defined as follows:

$$\tau_f = \frac{f_{85} - f_{25}}{60 \times f_{25}} \times 10^6 (\text{ppm}/^\circ\text{C}) \quad (1)$$

where  $f_{85}$  and  $f_{25}$  represent the resonant frequencies at  $85^\circ\text{C}$  and  $25^\circ\text{C}$ , respectively.

### 3. Results and discussion

The XRD patterns of  $\text{Li}_2\text{MgZrO}_4$  samples sintered at  $1125\text{-}1225^\circ\text{C}$  were shown in Fig. 1(a). It was clearly understood from this figure that all the compositions form a solid solution with rock-salt structure and I41/amd space group (No. 141  $Z=2$ ). Diffraction peaks of predominant phase gradually increased with the sintering temperature. In addition, secondary phases of  $\text{ZrO}_2$  with monoclinic structure were observed at  $28\text{-}32^\circ$  in the range of  $1200\text{-}1225^\circ\text{C}$ . Y. Iida et al. previously reported that the volatile content of lithium element was negligibly small under  $1000^\circ\text{C}$  and become larger at higher temperatures [15]. Thus, it was considered that evaporation of lithium was the major factor in the formation of the second phase above  $1175^\circ\text{C}$ . Rietveld refinement analysis of the ceramics sintered at  $1175^\circ\text{C}$  was shown in Fig. 1(b). Rietveld discrepancy factors  $R_p$ ,  $R_{wp}$  and  $R_{exp}$  were 5.86%, 8.72% and 2.34%, respectively. Schematic representation of single Mg/Zr-O octahedral was also shown in the inside of Fig. 1(b). Lattice parameters were calculated as  $a=b=4.19471\text{\AA}$ ,  $c=9.1686\text{\AA}$  and  $V=161.3270\text{\AA}^3$ , which were used to calculate the bond length and nature of bonding in the following section.

Fig. 2(a) illustrated the variation of the apparent densities and diametric shrinkage ratio of  $\text{Li}_2\text{MgZrO}_4$  ceramics with sintering temperature. The apparent densities gradually increased from 2.98 to  $3.33\text{ g/cm}^3$  with the sintering temperature

increasing from 1125-1225°C and reached a value of 3.15 g/cm<sup>3</sup> at 1175°C. The shrinkage ratio showed a similar tendency that increased from 5.35% to 8.15% and reached 7.05% at 1175°C. The apparent density of the sample sintered at 1175°C was 79.02% of its theoretical densities. This lower relative density would be harmful for improving microwave dielectric properties of Li<sub>2</sub>MgZrO<sub>4</sub> ceramics. The SEM micrographs of Li<sub>2</sub>MgZrO<sub>4</sub> ceramics sintered at different temperatures were illustrated in Fig. 3. The grain size of the ceramics gradually increased and much pores existed in samples sintered at 1125-1175°C. Clear grain boundaries and a small amount pores could be observed in Fig 3(a)-(c). However, the sintering at 1200 and 1225°C led to indistinct-grained Li<sub>2</sub>MgZrO<sub>4</sub> ceramics with irregular grain diameter and shapes. Moreover, as shown in Fig. 3(e), abnormal grain growth was observed and partial grains began to melt, which would have a detrimental effect on the  $Q \cdot f$  value. Due to the evaporation of lithium, an appreciable amount of intergranular pores was still existed in Fig. 3(e)-(f), which was in good agreement with the lower apparent densities shown in Fig. 2(a).

The variation of microwave dielectric properties of Li<sub>2</sub>MgZrO<sub>4</sub> ceramics was shown in Fig. 2(b). It was found that the dielectric constant gradually increased from 11.14 to 13.12 with the increase of sintering temperature from 1125 to 1225°C, and then reached to 12.30 at 1175°C. In order to eliminate the impact of porosity, the porosity-corrected permittivity ( $\epsilon_{rc}$ ) was calculated as Equ. 2:

$$\frac{\epsilon_r - \epsilon_{rc}}{3\epsilon_r} = \frac{\delta(\epsilon_1 - \epsilon_{rc})}{\epsilon_1 + 2\epsilon_r} \quad (2)$$

where  $\epsilon_r$  was the measured dielectric constant,  $\epsilon_1$  was dielectric constant of porosity,  $\delta$  was the fractional porosity. To clarify effects of crystal structure on dielectric constant, theoretical dielectric polarizability ( $\alpha_{\text{theo.}}$ ) was calculated to be 15.01 according to additive rule with ionic polarizability of composing ions or oxides [16]. Whereas the observed dielectric polarizability ( $\alpha_{\text{obs.}}$ ) of the ceramics sintered at 1175°C was calculated to be 16.23 by Clausius-Mossotti equation with the porosity-corrected permittivity [17]. By comparison, the values of  $\alpha_{\text{theo.}}$  and  $\alpha_{\text{obs.}}$  were in agreement with each other, and the deviation from the  $\alpha_{\text{theo.}}$  and  $\alpha_{\text{obs.}}$  was attributed to the evaporation of lithium.

The  $Q \cdot f$  values gradually increased from 27,600 to 40,900 GHz with the sintering temperature increasing from 1125 to 1175°C and reached a maximum value at 1175°C. However, the values significantly reduced to 21,500 GHz when the sintering temperature was higher than 1175°C. Combining with the results shown in Fig. 1(a) and Fig. 3(d), it could be concluded that the poor microstructure and the appearance of second phase led to the low  $Q \cdot f$  values at 1200°C. Although the ceramics got densified and the  $Q \cdot f$  values increased to 28,100 GHz at 1225°C, it was considered that the formation of second phases still played an important role in increasing the dielectric loss. In addition, it was well known that intrinsic losses were mainly caused by crystal structure such as bond strength and bond energy. Shorter bond length was correlated with higher bond energy, and higher bond energy could make the system more stable [18]. Sanderson reported that the bond energy could be obtained by the chemical bond and the electronegativity [19-21]. Based on the previous

researches, the bond energy  $E$  of the  $\text{Li}_2\text{MgZrO}_4$  ceramics sintered at  $1175^\circ\text{C}$  were calculated as Equ. 3-5 and the results were shown in Table 1.

$$E = \sum_{\mu} E_b^{\mu} \quad (3)$$

$$E_b^{\mu} = t_c E_c^{\mu} + t_i E_i^{\mu} \quad (4)$$

$$E_c^{\mu} = \frac{(r_{cA} + r_{cB})}{d^{\mu}} (E_{A-A} E_{B-B})^{1/2} \quad (5)$$

As shown in Table 1, total covalent energies ( $E_c$ ) and ionicity energies ( $E_i$ ) were 4024.7190 and 11659.2200  $\text{kJ mol}^{-1}$ . There was a sequence of bond energy of  $E_{\text{ave}}(\text{Zr-O}) > E_{\text{ave}}(\text{Li-O}) > E_{\text{ave}}(\text{Mg-O})$ . Some reports also investigated that the bond energy between the octahedral-site cation and oxygen would affect the  $Q \cdot f$  values [22, 23]. Thus, bond energy of  $E(\text{Zr-O})$  took the predominant role in  $\text{Li}_2\text{MgZrO}_4$  ceramics. Moreover, the  $\tau_f$  values fluctuated from -12.57 to -15.68  $\text{ppm}/^\circ\text{C}$  with the sintering temperatures increasing from 1125 to  $1225^\circ\text{C}$ , which would possibly make the ceramics more applicable for microwave devices.

#### 4. Conclusion

Ultra-low loss  $\text{Li}_2\text{MgZrO}_4$  ceramics were successfully synthesized by the conventional solid-state route. Crystal structure, sintering characteristics and microwave dielectric properties were discussed. Secondary phases and evaporation of lithium were observed when sintering temperatures exceeded  $1175^\circ\text{C}$ . Dielectric constant was strongly dependent on the porosity and polarizability.  $Q \cdot f$  values were mainly affected by microstructure under  $1175^\circ\text{C}$ , and second phase played an important role above  $1175^\circ\text{C}$ .  $\tau_f$  values fluctuated from -12.57 to -15.68  $\text{ppm}/^\circ\text{C}$  with sintering temperature increasing. Moreover, the theory of the bond energy was used to analysis the variation of  $Q \cdot f$  values. The excellent microwave property of  $\text{Li}_2\text{MgZrO}_4$  ceramics was found at  $1175^\circ\text{C}$  with  $\epsilon_r=12.30$ ,  $Q \cdot f=40,900$  GHz and  $\tau_f=-12.31$   $\text{ppm}/^\circ\text{C}$ , which would make the ceramics promising for application in microwave components.

#### Acknowledgments

This work was supported by the National Training Plan Innovation Project of college students (No.201510427001) and National Natural Science Foundation (No. 51472108).

#### Reference

- [1] S. Nishigaki, H. Kato, S. Yano, R. Kamimure, Am. Ceram. Soc. Bull. 66 (1987) 1405-1410.
- [2] K. Wakino, K. Minai, H. Tamura, J. Am. Ceram. Soc. 67 (1984) 278-281.
- [3] T. Takada, S.F. Wang, S. Yoshikawa, S.J. Jang, R.E. Newnham, J. Am. Ceram. Soc. 77 (1994) 1909-1916.
- [4] J.K. Plourde, D.F. Linn, H.M.J. O'Bryan, J.J. Thompson, J. Am. Ceram. Soc. 58 (1975) 418-420.

- [5] P. Zhang, Z.K. Song, Y. Wang, Y.M. Han, H.L. Dong, L.X. Li, J. Alloy. Compd. 581 (2013) 741-746.
- [6] P. Zhang, J. Liu, Y.G. Zhao, H.Y. Du, X.Y. Wang, Mater. Lett. 162 (2016) 173-175.
- [7] Z.F. Fu, P. Liu, J.L. Ma, X.M. Chen, H.W. Zhang, Mater. Lett. 164 (2016) 436-439.
- [8] P. Zhang, Y. Wang, J. Liu, Z.K. Song, Y.M. Han, L.X. Li, Mater. Lett. 123 (2016) 195-197.
- [9] Y.W. Tseng, J.Y. Chen, Y.C. Kuo, C.L. Huang, J. Alloys. Compd. 509 (2015) L308-L310.
- [10] G.G. Yao, X.S. Hu, X.L. Tian, P. Liu, J.P. Zhou, Ceram. Int. 41 (2015) S563-S566.
- [11] M. Castellanos, A.R. West, W.B. Reid, Acta Cryst. C 41 (1985) 1707-1709.
- [12] E.S. Kim, C.J. Jeon, P.G. Clem, J. Am. Ceram. Soc. 95 (2012) 2934-2938.
- [13] B.W. Hakki, P.D. Coleman, IEEE Trans. Microwave. Theory Tech. 8 (1960) 402-410.
- [14] W.E. Courtney, IEEE Trans. 18 (1970) 476-485.
- [15] Y. Iida, J. Am. Ceram. Soc. 43 (1960) 171-172.
- [16] R.D. Shannon, G.R. Rossman, Am. Miner. 77 (1992) 94-100.
- [17] R.D. Shannon, J. Appl. Phys. 73 (1993) 348-366.
- [18] S.D. Ramarao, V.R.K. Murthy, Dalton Trans. 44 (2015) 2311-2324.
- [19] R.T. Sandderson, Inorg. Nucl. Chem. 30 (1968) 375-393.
- [20] R.T. Sandderson, Academic Press: New York 1971.
- [21] R.T. Sandderson, J. Am. Chem. Soc. 105 (1983) 2259-2261.
- [22] H.T. Wu, E.S. Kim, J. Alloy. Compd. 669 (2016) 134-140.
- [23] P. Zhang, Y.G. Zhao, H.T. Wu, Dalton Trans. 44 (2015) 16684-16693.

Fig. 1 (a) XRD patterns of  $\text{Li}_2\text{MgZrO}_4$  ceramics sintered at 1125-1225°C for 4 h. (b) Rietveld refinement of  $\text{Li}_2\text{MgZrO}_4$  ceramics ( $R_p=5.86\%$ ,  $R_{wp}=8.72\%$ ,  $R_{\text{exp}}=2.34\%$ ) and schematic representation of single Mg/Zr-O octahedral.

Fig. 2 (a) Apparent densities and shrinkage ratio of  $\text{Li}_2\text{MgZrO}_4$  ceramics as a function of sintering temperatures from 1125 to 1225°C. (b) Curves of  $\epsilon_r$ ,  $Q \cdot f$  and  $\tau_f$  values as a function of sintering temperatures for  $\text{Li}_2\text{MgZrO}_4$  ceramics in the temperature region of 1125-1225°C.

Fig. 3 SEM micrographs of  $\text{Li}_2\text{MgZrO}_4$  ceramics sintered at different temperatures for 4 h (a-e corresponding to 1125°C, 1150°C, 1175°C, 1200°C and 1225°C).

Table 1 Calculation of bond energy of  $\text{Li}_2\text{MgZrO}_4$  ceramics sintered at 1175 °C.

Bond Type	<i>d</i>	Electronegativity of cations	Ion coefficient	Covalent coefficient	Covalent radius of cations	Total of covalent radius	A site bond (kJ/mol)	B site bond (kJ/mol)	<i>E<sub>c</sub></i> (kJ/mol)	<i>E<sub>i</sub></i> (kJ/mol)	<i>E</i> (kJ/mol)
Li-O(1)× <sub>4</sub>	2.103 <sub>7</sub>								213.127 <sub>0</sub>	659.9914	396.341 <sub>4</sub>
		0.98	0.4100	0.5900	133	196	105.00 <sub>00</sub>	498.36 <sub>00</sub>			
Li-O(2)× <sub>2</sub>	2.455 <sub>0</sub>								182.629 <sub>5</sub>	565.5495	339.626 <sub>7</sub>
Mg-O(1)× <sub>4</sub>	2.103 <sub>7</sub>								72.0574	659.9914	280.774 <sub>0</sub>
		1.31	0.3550	0.6450	139	202	11.300 <sub>0</sub>	498.36 <sub>00</sub>			
Mg-O(2)× <sub>2</sub>	2.129 <sub>3</sub>								71.1910	652.0565	277.398 <sub>3</sub>
Zr-O(1)× <sub>4</sub>	2.103 <sub>7</sub>								397.650 <sub>3</sub>	659.9914	489.907 <sub>0</sub>
		1.33	0.3517	0.6483	154	217	298.20 <sub>00</sub>	498.36 <sub>00</sub>			
Zr-O(2)× <sub>2</sub>	2.129 <sub>3</sub>								392.869 <sub>5</sub>	652.0565	484.016 <sub>9</sub>
Total	—	—	—	—	—	—	—	—	4024.71 <sub>90</sub>	11659.22 <sub>00</sub>	6870.17 <sub>34</sub>

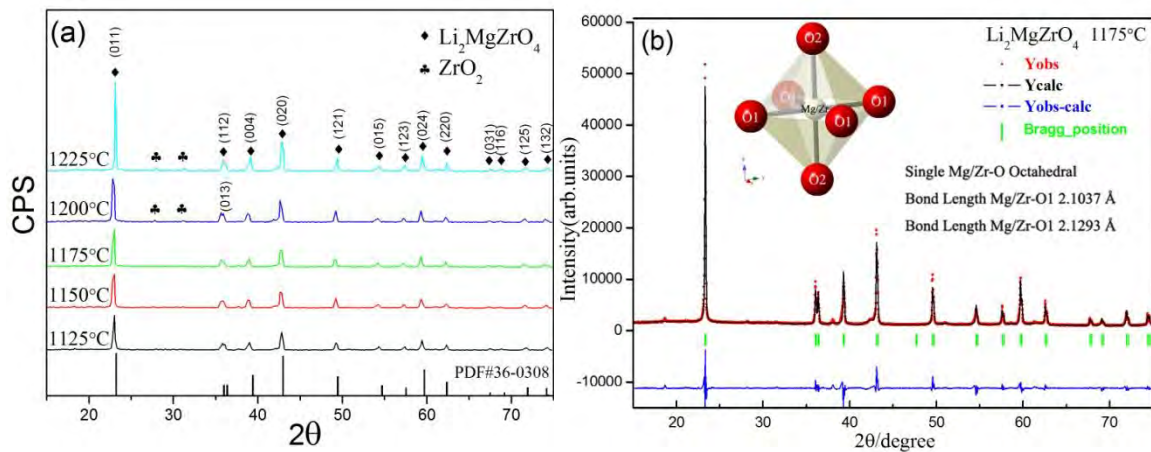


Fig. 1

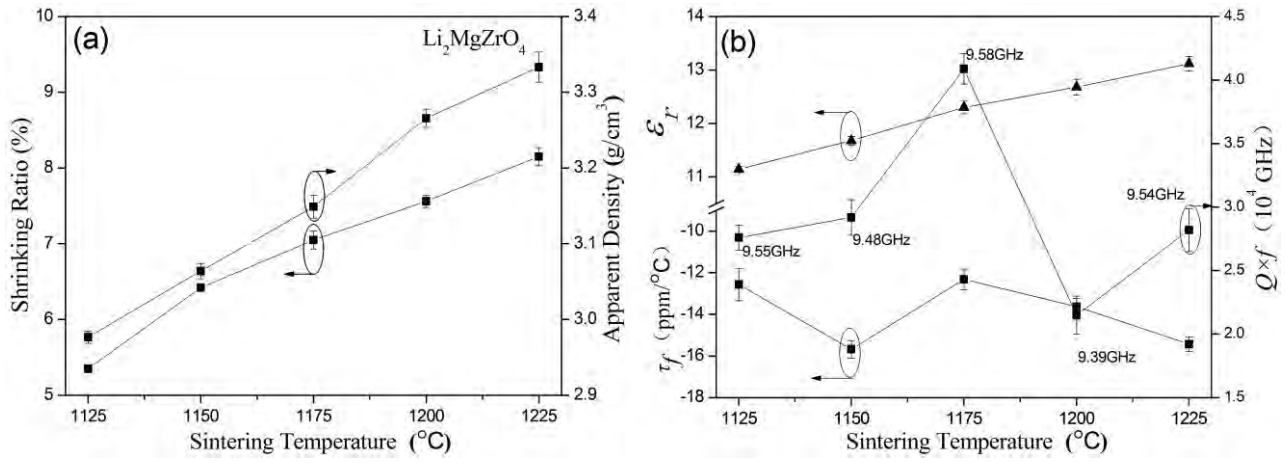


Fig. 2

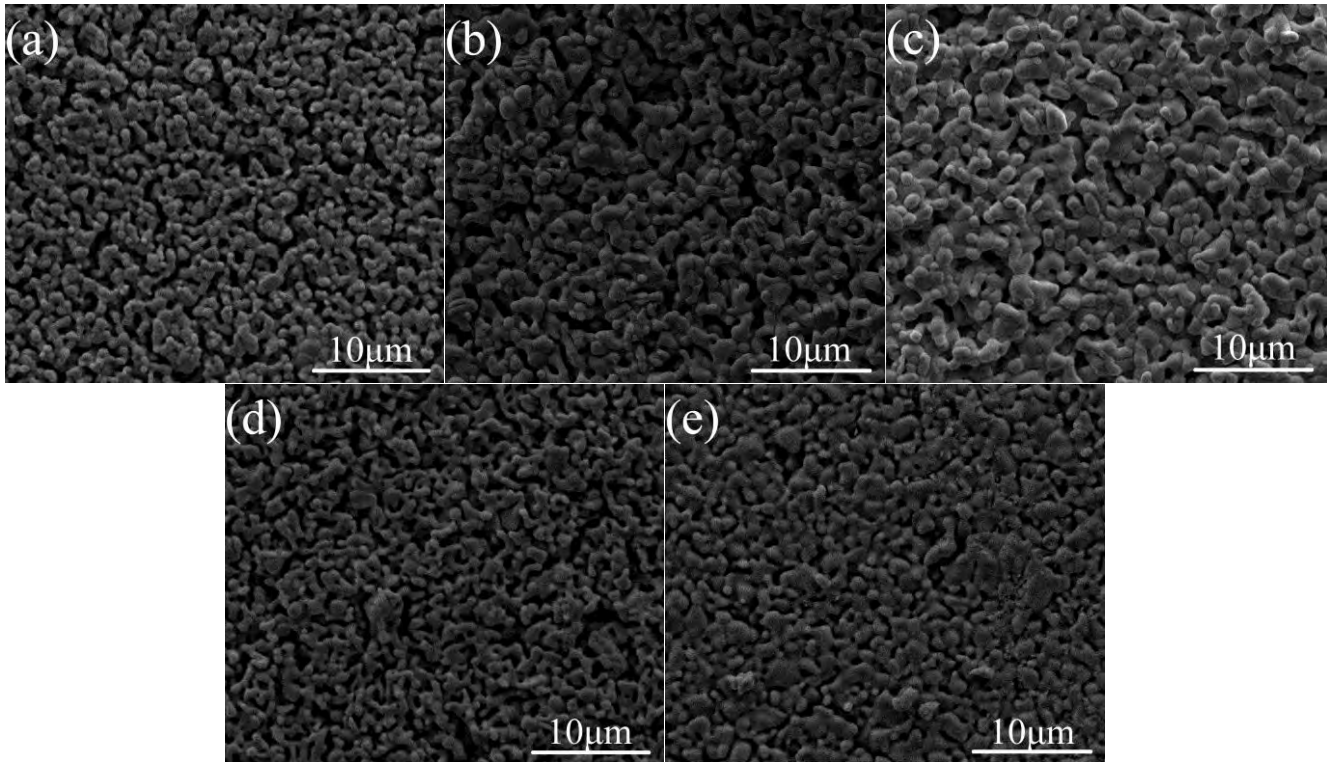


Fig. 3

## Highlights

- New rock-salt structure  $\text{Li}_2\text{MgZrO}_4$  were reported with good microwave properties
- The ceramics exhibited properties with  $\epsilon_r=12.30$ ,  $Q \cdot f = 40,900$  GHz  $\tau_f = -12.31$  ppm/°C.
- Bond energy of ceramics was reported for first time to analyze intrinsic loss.